Indian Journal of Pure & Applied Physics
Vol. 58, July 2020, pp. 558-568

Influence of Soret and Dufour effect on MHD flow over an exponential stretching sheet: A numerical study

Seema Tinker[a], S R Mishra[b] & Ram Prakash Sharma[c*]

[a]Department of Mathematics, JECRC University Jaipur 303 905, India

[b]Department of Mathematics, Siksha 'O' Anusandhan Deemed to be University, Khandagiri, Bhubaneswar 751 030, India

[c]Department of Mechanical Engineering, National Institute of Technology, Arunachal Pradesh, Yupia, Papum Pare District 791 112, India

Received 8 January 2020; accepted 2 June 2020

The present paper analyzes the effect of chemical reaction on free convection MHD motion of steady, laminar, incompressible liquid under the influence of heat source/sink. The motion is considered over an exponential radiative extending surface with a magnetic field. An appropriate similar transformation is employed to convert the nonlinear system of partial differential equations (PDEs) to a set of ordinary differential equations (ODEs). Due to the high nonlinearity, the analytical approach for these coupled nonlinear equations does not hold good. Therefore, these transformed ODEs are solved by using numerical techniques adopting Runge-Kutta fourth-order method accompanied by shooting technique. The behavior of different physical parameters on the motion phenomena is shown via diagrams. However, as a concluding remark, the major outcomes of the present investigation are described as: the buoyant forces overshoot the velocity profile significantly whereas the fluid temperature retards with an increasing Soret number. Finally, the chemical reaction parameter favors retard the concentration profiles resulted in reducing the thickness of the solutal boundary layer.

Keywords: MHD, Buoyant forces, Soret and Dufour effect, Thermal radiation

1 Introduction

Viscous fluid motion and the interaction of the magnetic field constituent a significant mechanical problem associated with the various applied field of science and technology along with industrial uses. Therefore, now a days, researchers around any corner of the world have contributed their research on the same field for the development in the properties of the flow phenomena which helps in many directions to the society. Some of the industrial applications are metallic spinning, dissimilar extrusions like polymer and metals, and wires drawing.

In various heat and concentration transport issues, the outcome of diffusion thermo and thermal diffusion impacts are disregarded viz. Cortell[1,2], Ibrahim[3] and Shateyi[4,5], the reason behind it that the magnitude is smaller than the impacts reported by Fick's and Fourier's laws. The Ludwig-thermal diffusion impact corresponds to species separation expanding in beginning uniform assortment focused on a heat gradient. The temperature flux impelled through a mass gradient is described Dufour effect. These impacts are examined as subsequent order phenomenon and are remarkable in fields, for instance, chemical reactor, water, petrology, drying procedures, geosciences, etc. Initially, Sakiadis[6] has applied boundary layer motion past a rotating expending surface where velocity is taken as constant. Sakiadis derived the two dimensional boundary layer equations for axis-symmetric motion. Karthikeyan[7] has analyzed the influence of transfer of energy and concentration in the existence of internal energy generation, diffusion thermo impact, and thermal radiation in an unstable magnetohydrodynamic stagnation point motion in the direction of a vertical sheet inserted in a permeable media in mixed convection. Reddy and Chamkha[8] have emphasized the study of properties of concentration and energy transfer of an unstable magnetohydrodynamic boundary layer motion in a permeable media in the existence of Soret and thermo-diffusion outcomes under the influence of thermal radiation, thermophoresis and uneven heat sink /source past a stretching sheet. The slowdown in velocity, temperature and concentration profiles is noted here because the suction moves the warm liquid away from the sheet of the stretching film.

*Corresponding author (E-mail: rpsharma@nitap.ac.in)

Gbadeyan *et al.*[9] have focused the dilemma of coupled mass and heat transport by natural convective of an incompressible viscous liquid electrically and chemically reactive, defined by a corrugated wall and a plain wall with Soret effect and an internal energy source/sink. Bhattacharyya *et al.*[10] have presented a mathematical representation to examine the impact of Dufour effect and thermo diffusion on the transport of energy and concentration convection in a flow stagnation position of an incompressible viscous liquid to a surface in contraction. Double solutions of energy and concentration are acquired with the above effects. Also, there is a double crossover in the dimensionless heat descriptions for enhancing the thermo diffusion number and in the two-dimensional growth mass descriptions for increasing the diffusion thermo number. The analysis shows that the numbers of Dufour effect and thermo diffusion powerfully influence the transfer phenomenon.

Mishra *et al.*[11] reported the impact of Soret and chemical reaction on magnetohydrodynamic micropolar liquid over an extending surface. Sharma and Mishra[12] studied the outcome of Soret and diffusion thermo effect on MHD micropolar fluid flow. Sharma *et al*[13] explored the outcome of chemical reaction on magnetohydrodynamic rotating liquid over a vertical surface. Shamshuddin *et al*[14] have reported the chemically reacting micropolar liquid over a porous extending surface.

Chamkha *et al*[15] reported the influences of thermo diffusion and diffusion thermo on the convective energy and concentration transport motion via a permeable media in a rectangular canal in the inclined magnetic field. Zheng *et al.*[16] have examined the unstable energy and concentration transport of a dual dimensional magnetohydrodynamic liquid on a rotating oscillating extending surface under the control of diffusion thermo and Soret effects. The internal friction effects are taken over into the heat equation. In the flow way, an identical magnetic field is applied vertically. Bishwa *et al.*[17] have examined the outcomes in a porous medium of Soret, Dufour, and energy source, on the run of the magnetohydrodynamic laminar on a non-insulated stretch sheet. The mass and heat transfer properties of the magnetohydrodynamic forced convective motion on a non-isothermal stretched film inserted in a permeable media exposed to a heat source are studied numerically where the influence of Soret and Dufour are taken into account. The mass transfer rate reduces with rising permeability parameter, Soret number, magnetic field parameters, and thermal stratification parameter, but enhances with rising heat source parameter and Dufour number.

Uwanta and Usman[18] have reported the cumulative impact of Soret and Dufour effect on natural convection energy and mass transport to the unstable laminar motion in a vertical canal with internal friction and steady suction. In this work, the influence of thermo diffusion and diffusion thermo on the energy and mass transport by free convective of MHD in a vertical channel with constant viscous suction and discharge is investigated. The movement of the incompressible viscous liquid via a permeable media under the impact of heat and concentration transfer on a shrinking sheet with transverse diffusion impact between energy and concentration has been reported by Eldabe *et al.*[19]. To study the influences of Soret and diffusion thermo on energy and mass transport with variable viscosity over a vertical surface was studied by Moorthy *et al.*[20].

Vedavathi *et al.*[21] have discussed the influences of energy and mass transport on a dual-dimensional, unstable magnetohydrodynamic natural convective motion across a vertical porous sheet in a permeable media with subsurface energy radiation and effect of diffusion thermo and thermo diffusion. Sharma *et al.*[22] have described the influence of Soret on the convection motion of magnetohydrodynamic via a permeable media over a vertical sheet in the influence of chemical reaction, radiation, and energy source/sink. The deposition of free thermophores particles convection embedded on a vertical sheet in a flooded liquid in the non-Darcy permeable media was examined by Partha[23]. The behavior of both the Soret and Dufour effects on the two-dimensional time-dependent flow past a semi-infinite vertical porous plate has been investigated by Shivaiah and Rao[24].

A limited number of other studies on assorted flow over a curved surface subject to Soret and Dufour effects are given in references[25–28]. Hsiao *et al.*[29] have mathematically observed the collective impact of energy and concentration transport of a non-Newtonian power law, conductive liquid, in natural convective magnetohydrodynamic nearby to a vertical surface in a porous media with the evidence of thermophores particles impact. The results of thermo diffusion and Dufour impact on the energy and mass transport was explored by Chapman *et al.*[30].

Come across several earlier discussions we aim to contribute to the motion of an electrically conducting free convective viscous fluid over an exponentially extending surface. Moreover, for the enhancement of properties of flow phenomena, the influence of buoyant forces such as both the thermal and solutal buoyancy on the velocity descriptions, the additional heat source/sink and Dufour number in the energy equation, impact of thermo diffusion on the mass transport equation have also taken care of. These physical quantities play a vital role. Finally, the transformed complex set of equations is solved numerically and the behavior of pertinent parameters is presented via graphs. The numerical validation is obtained in comparison to earlier studies through tabulated values and concluding remarks for the discussion are also presented.

2 Problem Formalism

The steady 2-D motion of conducting viscous liquid past an exponentially extending surface has been considered in the present investigation. The influence of chemical reaction is also taken care of in the mass transfer equation. The surface is along the direction of the x-axis where the flow takes place and the y-axis is transverse to it. The surface and ambient temperature of the sheet is assumed to be T_w and T_∞ whereas the solutal concentration is assumed to be C_w and C_∞ respectively (Fig. 1). A variable magnetic field $B(x)$ is acting normal to the surface and the induced magnetic field is considered as very negligible with a small value of magnetic Reynolds number. The governing non-dimensional equations are considered as:

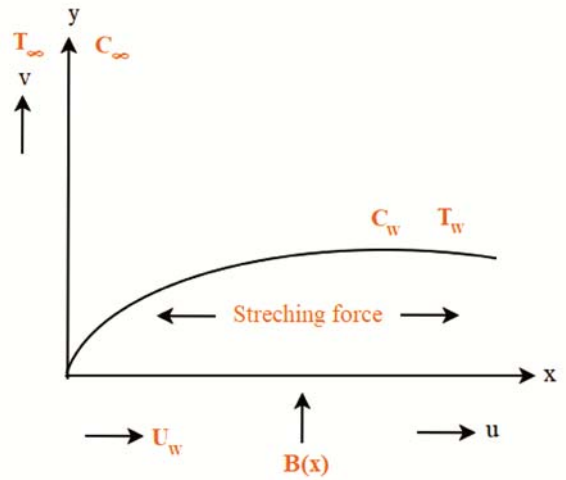

Fig. 1 — Schematic diagram of a flow problem.

$$\frac{\partial \tilde{u}}{\partial x}+\frac{\partial \tilde{v}}{\partial y}=0 \quad \ldots (1)$$

$$\tilde{u}\frac{\partial \tilde{u}}{\partial x}+\tilde{v}\frac{\partial \tilde{u}}{\partial y}=\upsilon\frac{\partial^2 \tilde{u}}{\partial y^2}-\frac{\sigma B^2(x)}{\rho}\tilde{u}+g\beta_C(\tilde{C}-\tilde{C}_\infty)+g\beta_T(\tilde{T}-\tilde{T}_\infty) \quad \ldots(2)$$

$$\tilde{u}\frac{\partial \tilde{T}}{\partial x}+\tilde{v}\frac{\partial \tilde{T}}{\partial y}=\alpha\frac{\partial^2 \tilde{T}}{\partial y^2}-\frac{1}{\rho\tilde{C}p}\frac{\partial q_r}{\partial y}+\frac{D_m\kappa_T}{\tilde{C}s\tilde{C}p}\frac{\partial^2 \tilde{C}}{\partial y^2}+\frac{Q_0}{\rho\tilde{C}p}\left(\tilde{T}-\tilde{T}_\infty\right) \quad \ldots(3)$$

$$\tilde{u}\frac{\partial \tilde{C}}{\partial x}+\tilde{v}\frac{\partial \tilde{C}}{\partial y}=D\frac{\partial^2 \tilde{C}}{\partial y^2}-k_c^{*}(\tilde{C}-\tilde{C}_\infty)+\frac{D_m\kappa_T}{\tilde{T}_m}\frac{\partial^2 \tilde{T}}{\partial y^2} \quad \ldots(4)$$

Following the Rosseland approximation[26,27], we have,

$$q_r=-\frac{4\sigma}{3k*}\frac{\partial \tilde{T}^4}{\partial y},\tilde{T}^4=4\tilde{T}_\infty^3\tilde{T}-3\tilde{T}_\infty^4 \quad \ldots(5)$$

So from equation (5),

$$\frac{\partial q_r}{\partial y}=-\left(\frac{16\sigma\tilde{T}_\infty^3}{3k^{*}}\right)\frac{\partial^2 \tilde{T}}{\partial y^2} \quad \ldots(6)$$

which reduces eq. (3) as,

$$\tilde{u}\frac{\partial \tilde{T}}{\partial x}+\tilde{v}\frac{\partial \tilde{T}}{\partial y}$$
$$=\alpha\frac{\partial^2 \tilde{T}}{\partial y^2}+\frac{16\tilde{T}_\infty^3\sigma}{3\rho\tilde{C}pk^{*}}\frac{\partial^2 \tilde{T}}{\partial y^2}+\frac{D_m\kappa_T}{\tilde{C}s\tilde{C}p}\frac{\partial^2 \tilde{C}}{\partial y^2}+\frac{Q_0}{\rho\tilde{C}p}\left(\tilde{T}-\tilde{T}_\infty\right) \quad \ldots(7)$$

The boundary conditions (as in reference[2]),

$$\left.\begin{aligned}&\tilde{u}=U_w(x),\tilde{v}=0,\tilde{C}=\tilde{C}_w=\tilde{C}_\infty+\tilde{C}_0\exp\left|\frac{x}{2L}\right|\\&\tilde{T}=\tilde{T}_w=\tilde{T}_\infty+\tilde{T}_0\exp\left|\frac{x}{2L}\right|,\text{ at } y=0\\&\tilde{u}\to 0,\ \tilde{C}\to\tilde{C}_\infty,\tilde{T}\to\tilde{T}_\infty,\text{ as y}\to\infty\end{aligned}\right\} \quad \ldots(8)$$

The magnetic field can be considered as

$$B(x)=B_0\exp\left|\frac{x}{2L}\right|$$

Establishing the stream function ψ :

$$\tilde{u} = \frac{\partial \psi}{\partial y} \text{ and } \tilde{v} = -\frac{\partial \psi}{\partial x}. \quad \ldots(9)$$

Using the following transformations with a similarity variable (η),

$$\left.\begin{aligned} &\tilde{u} = U_0 f'(\eta)\exp\left|\frac{x}{L}\right|, \tilde{v} = -\sqrt{\frac{\nu U_0}{2L}}\{f(\eta)+\eta f'(\eta)\}\exp\left|\frac{x}{2L}\right| \\ &\eta = \sqrt{\frac{U_0}{2\nu L}} y \exp\left|\frac{x}{2L}\right|, \tilde{C} = \tilde{C}_\infty + \tilde{C}_0 \exp\left|\frac{x}{2L}\right|\phi(\eta), \\ &\tilde{T} = \tilde{T}_\infty + \tilde{T}_0 \exp\left|\frac{x}{2L}\right|\theta(\eta) \end{aligned}\right\} \quad \ldots(10)$$

Equations (2),(4) and (7) reduced to:

$$f''' + ff'' - 2ff' - Mf' + \lambda_1\theta + \lambda_2\phi = 0 \quad \ldots(11)$$

$$\frac{1}{\Pr}\left(1+\frac{4}{3}R\right)\theta'' + (f\theta' - f'\theta) + Du\phi'' + Q\theta = 0 \quad \ldots(12)$$

$$\phi'' + ScSr\theta'' + Sc(f\phi' - f'\phi) - ScKc\phi = 0 \quad \ldots(13)$$

The boundary conditions (8) convert as:

$$\left.\begin{aligned} &f(0)=0, f'(0)=1, f'(\infty)\to 0, \\ &\theta(0)=1, \theta(\infty)\to 0, \\ &\phi(0)=1, \phi(\infty)\to 0 \end{aligned}\right\} \quad \ldots(14)$$

Where

$$\alpha = \frac{k}{\rho\tilde{C}p}, M = \frac{2\sigma B_0^2 L}{\rho U_0}, \Pr = \frac{\upsilon}{\alpha}, R = \frac{4\sigma\tilde{T}_\infty^3}{kk^*},$$

$$Sc = \frac{D}{\nu}, Kc = \frac{k_c^*}{\exp\left|\frac{x}{L}\right|}, Q = \frac{Q_0}{\rho\tilde{C}_P}\frac{2L}{U_0}\frac{1}{\exp\left|\frac{x}{L}\right|}$$

$$Du = \frac{D_m\kappa_T}{\nu\tilde{C}s\tilde{C}p}\frac{(\tilde{C}-\tilde{C}_\infty)}{(\tilde{T}_w-\tilde{T}_\infty)}, Sr = \frac{D_m\kappa_T}{\nu\tilde{T}_m}\frac{(\tilde{T}_w-\tilde{T}_\infty)}{(\tilde{C}-\tilde{C}_\infty)}$$

3 Physical Quantities

The local skin friction, the Nusselt and Sherwood number are expressed as C_{fx}, Nu_x and Sh_x respectively. Where

$$C_{fx}\sqrt{\mathrm{Re}_x} = f''(0), \frac{Nu_x}{\sqrt{\mathrm{Re}_x}} = -\left(1+\frac{4}{3}R\right)\theta'(0),$$

$$\frac{Sh_x}{\sqrt{\mathrm{Re}_x}} = -\phi'(0)$$

and $\sqrt{\mathrm{Re}_x} = \frac{U_w x}{\nu}$ is the local Reynolds number.

4 Numerical computation

The transformed governing equations of ODEs (11) - (13) are converted to a set of ODEs and for which only four initial conditions are available. Because of the absence of initial conditions, the rest of the three initial conditions are assumed, and then to find out these three unknowns Newton-shooting technique is employed. Hence, to explain the set of equations with an adequate number of initial conditions numerical technique i.e. Runge-Kutta fourth-order technique is adopted following Bhatti *et al.*[31]. The iterative procedure will continue to get an accuracy of 10^{-6}. The algorithm is defined as:

Let

$$y_1 = f; y_2 = f'; y_3 = f''; y_4 = \theta; y_5 = \theta'; y_6 = \phi; y_7 = \phi'$$

Hence

$$y_3' = f''' = -y_3y_1 + 2y_2^2 + My_2 - \lambda_1 y_4 - \lambda_2 y_6 \quad \ldots(A)$$

$$y_5' = \theta'' = \frac{-\Pr[(y_1y_5 - y_2y_4) + Qy_4] - Du\Pr\left[Sc(y_2y_6 - y_1y_7) + ScKcy_6\right]}{\left[\left(1+\frac{4}{3}R\right) - Du\Pr ScSr\right]} \quad \ldots(B)$$

$$y_7' = \phi'' = \frac{\left[\begin{aligned} &\left(1+\frac{4}{3}R\right)\{-Sc(y_1y_7 - y_2y_6) + ScKcy_6\} \\ &-ScSr\{-\Pr(y_1y_5 - y_2y_4) - \Pr Qy_4\} \end{aligned}\right]}{\left[\left(1+\frac{4}{3}R\right) - Du\Pr ScSr\right]} \quad \ldots(C)$$

The expression for boundary conditions (9) is given as:

$$y_a(1)=0, y_a(2)=1, y_b(2)=s_1, y_a(4)=1,$$
$$y_b(4)=s_2, y_a(6)=1, y_b(6)=s_3 \quad \ldots(D)$$

where the suffixes a,b are the boundaries and the unknowns $s_1, s_2,$ and s_3 are to be determined.

5 Results and Discussion

We have presented the comprehensive solutions attained here in Figs 2-19. The problem numerically involves three fluid dynamic variables (f,θ,C), which are dependent on variable (η) and the parameters $M, \lambda_1, \lambda_2, R, Sr, Du, Sc, \Pr, Kc$ *and* Q, which are thermo-physical and control the body force. The following are the prescribed values of the default parameters, $M=1, \lambda_1=\lambda_2=0.5, Du=0.3, Sr=0.5,$ $\Pr=0.71, R=1, Kc=0.0, Q=0.5,$ and $Sc=0.22$.

At the time of computation, the values of characterizing parameters are treated as fixed except the variation of the parameters corresponding to different figures. We have obtained the computational outcome for different parameters here.

The impact of diverse parameters on the motion phenomena is determined and depicted. Figure 2 explains the reaction of M on the velocity outline with additional parameters used in the present analysis. We can see if M raises here, the velocity profile decreases. The cause behind this is the strength of the resistance. The conductive fluid creates a resistance due to Lorentz force in the presence of a magnetic field, which resists the run of momentum.

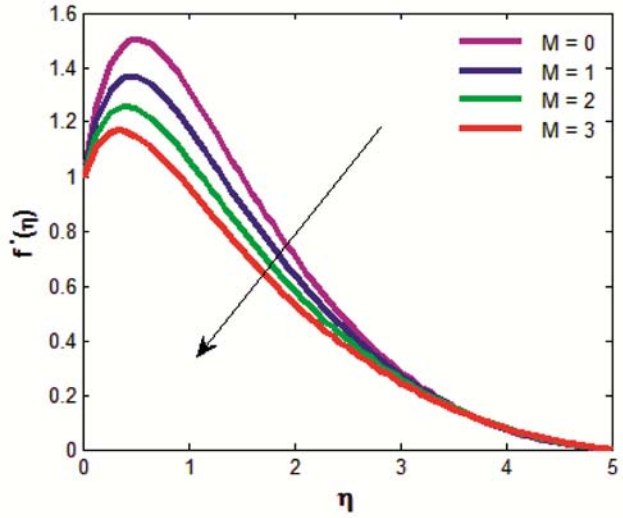

Fig. 2 — For dissimilar values of M the velocity outline of conductive fluid whileDu=0.3, Sr=0.5, Pr=0.71, R=1, Kc=0,Q=0.5, Sc=0.22, λ_1= λ_2=0.5.

Figure 3 demonstrates the reaction of λ_1 on the velocity distribution in the existence of heat source, magnetic parameter, buoyant solute, thermal radiation, and temperature-dependent *Kc*. As expected, arise in velocity due to arise in thermal buoyancy was observed. The positive value of λ_1 corresponds to the heat-repelling of the panel. Besides, as the value of λ_1 moves up, the velocity enhances quickly near the plate, so it is uniformly attenuated at the free flow momentum. The influence of local solutal buoyancy on the momentum distribution is shown in Fig. 4, in the existence of thermal buoyancy, heat source, magnetic parameters,

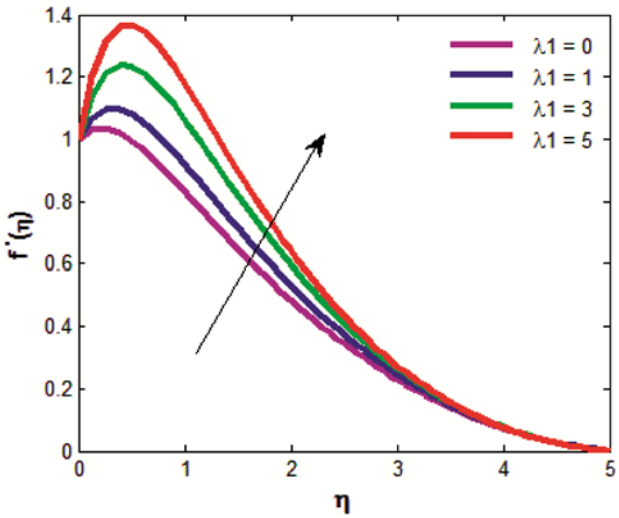

Fig. 3 — For dissimilar values of λ_1 the velocity distributionin which the values of thermo physical parameters are taken asM=1, Du=0.3, Sr=0.5, Pr=0.71, R=1, Kc=0,Q=0.5, Sc=0.22, λ_2=0.5.

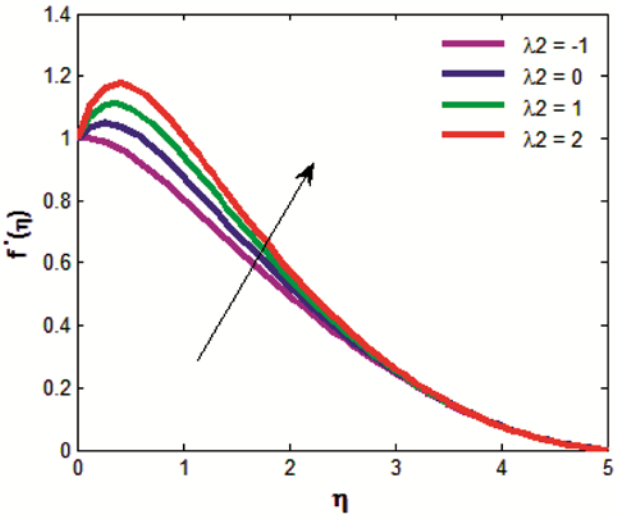

Fig. 4 — For distinct values of $\lambda_2$the velocity distributionin which the values of thermo physical parameters are taken as M=1, Du=0.3, Sr=0.5, Pr=0.71, R=1, Kc=0,Q=0.5, Sc=0.22, λ_1= 0.5.

chemical reaction parameters, and heat radiation which are functions of space and temperature. Grashof solute number λ_2 defines the relationship between the buoyancy of a species and viscous hydrodynamics. As expected, as the buoyancy of the species enlarges, the velocity of the fluid enlarges and the peaks are more unique. The reaction of the Dufour number on the momentum distribution is demonstrated in Fig. 5. When *Du* increases in the interval of $0 \leq Du \leq 2$, the velocity increases along with the vertical heating plate ($0 \leq \eta \leq 5$), and we also observe the initial velocity increase ($0 \leq \eta \leq 0.5$), and then the speed is continuously reduced. As can be seen from the figure, the reaction of the *Du* on the speed curve is not so considerable. The impact of the *Sc* on the momentum curve is revealed in Fig. 6. Schmidt's number reflects the relationship between mass diffusion and momentum. When Schmidt number raises its value, the fluid momentum reduces. Figure 7 shows the momentum outline for the distinct values of Q. The result explains that the influence of enhancing the value of the endothermic parameter leads to arise in momentum.

Figure 8 demonstrates the energy descriptions for distinct values of Pr which describes the relationship between the diffusivity of the moment and the thermal

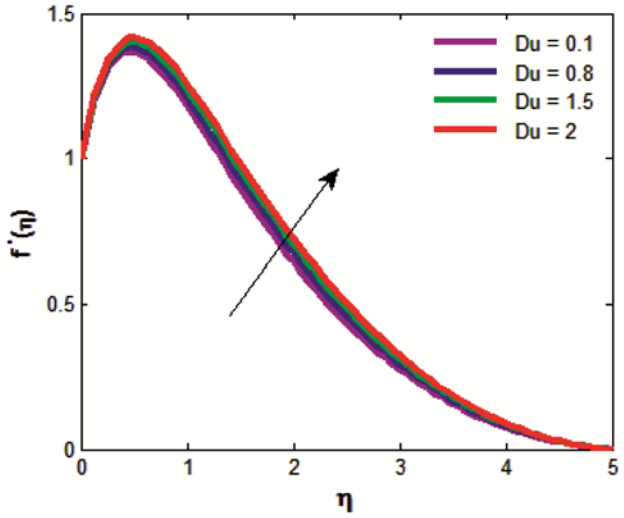

Fig. 5 — For dissimilar values of Du the velocity profilein which the values of thermo physical parameters are taken as M=1, Sr=0.5, Pr=0.71, R=1, Kc=0,Q=0.5, Sc=0.22, $\lambda_1 = \lambda_2 = 0.5$.

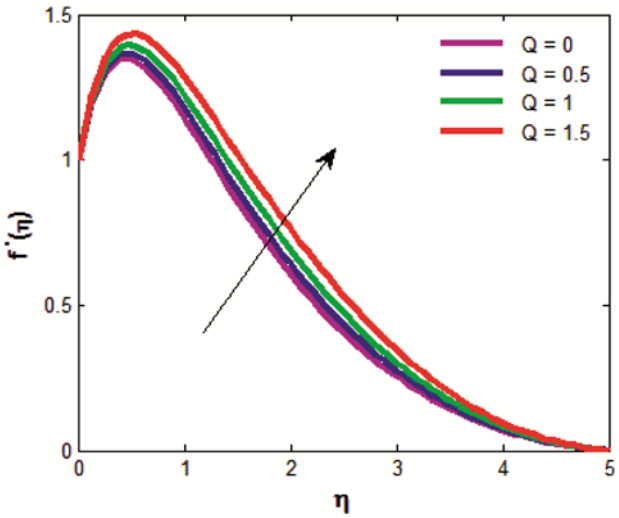

Fig. 7 — For dissimilar values of Q the momentum distributionin which the values of thermo physical parameters are taken as M=1, Du=0.3, Sr=0.5, Pr=0.71, R=1, Kc=0, Sc=0.22, $\lambda_1 = \lambda_2 = 0.5$.

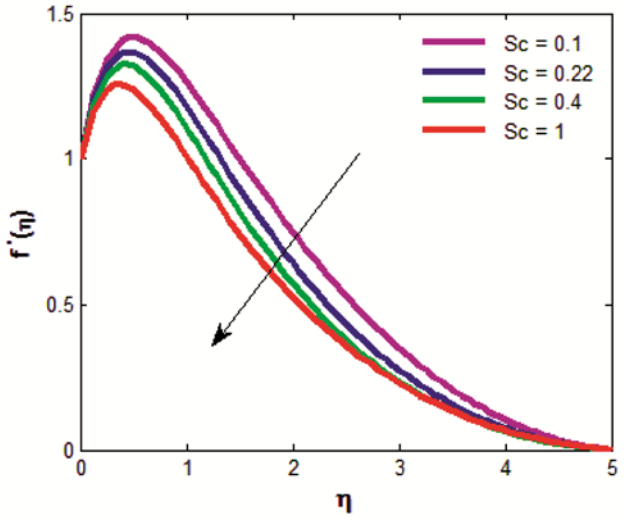

Fig. 6 — For distinct values of Sc the velocity distributionin which the values of thermo physical parameters are taken as M=1, Du=0.3, Sr=0.5, Pr=0.71, R=1, Kc=0, Q=0.5, $\lambda_1 = \lambda_2 = 0.5$.

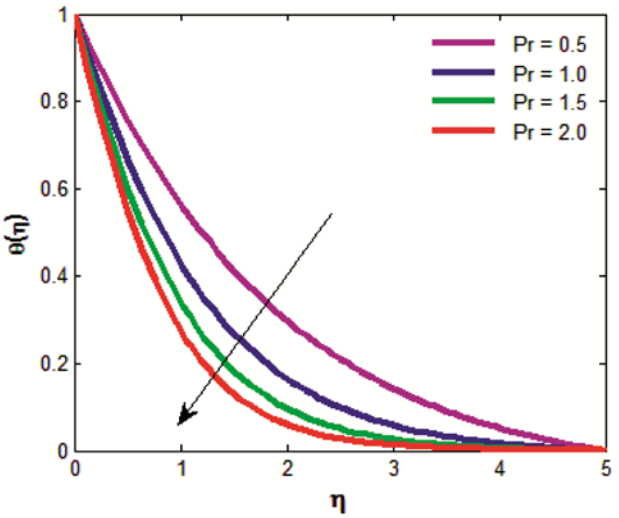

Fig. 8 — For distinct values of Pr the temperature profilein which the values of thermo physical parameters are taken as M=1, Du=0.3, Sr=0.5, R=1, Kc=0,Q=0.5, Sc=0.22, $\lambda_1 = \lambda_2 = 0.5$.

diffusivity. The increment in the value of Pr leads to a considerable reduction in the temperature inside the boundary layer. We can explain it as when Pr takes lower values, thermal conductivity increases, so that heat can be diffused faster from the heating surface in comparison to a higher Pr value and results in a lower mean temperature. Figure 9 shows the influence on heat profile for distinct values of the Dufour number Du. We can see that Du has a noteworthy effect on the temperature profile. It has been found that a raise in the Du affects the temperature of the entire boundary layer to rise and slowly decay from the surface to the free flow value.

Figure 10 illustrates the influence of distinct values of Soret number on temperature distribution. The value of Sr describes the outcome of the temperature gradient that causes considerable mass diffusion effects. Note that an enhancement in values of the thermo diffusion number shows a reduction in heat inside the boundary layer. The reaction of distinct values of the Schmidt number on the heat description is demonstrated in Fig. 11. Sc reflects the relationship between momentum and mass diffusion. The Schmidt number then quantifies the relative validity of the moment and the mass transfer of the diffusion inside the boundary layer. As the values of Sc enhance, the

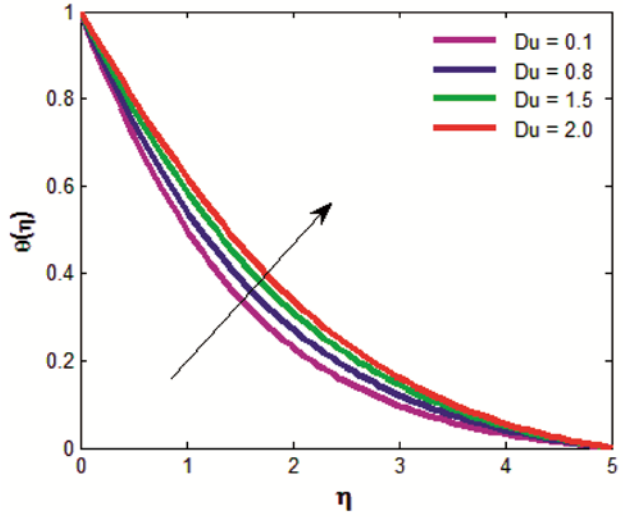

Fig. 9 — For distinct values of Du the temperature distributionin which the values of thermo physical parameters are taken as M=1, Sr=0.5, Pr=0.71, R=1, Kc=0, Q=0.5, Sc=0.22, λ_1= λ_2=0.5.

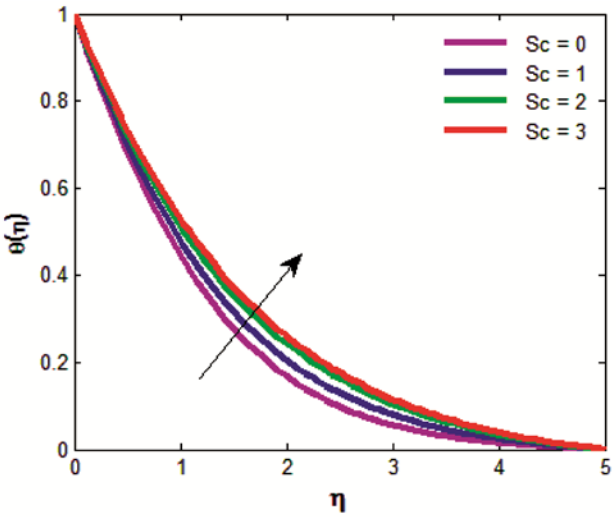

Fig. 11 — For distinct values of Sc the temperature profilein which the values of thermo physical parameters are taken as M=1, Du=0.3, Sr=0.5, Pr=0.71, R=1, Kc=0, Q=0.5, λ_1= λ_2=0.5.

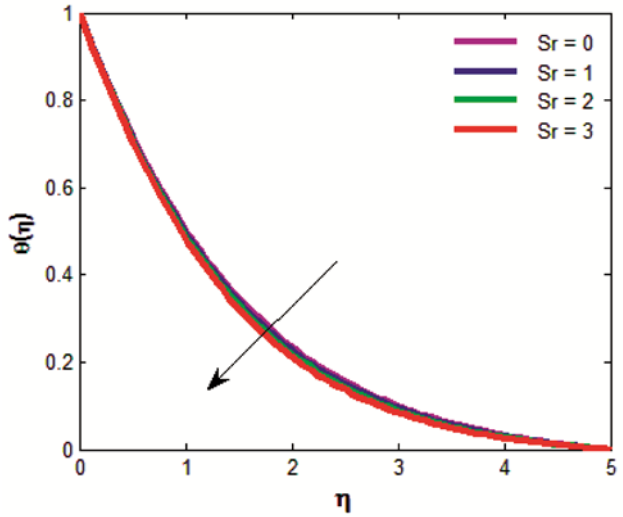

Fig. 10 — For distinct values of Sr the temperature distributionin which the values of thermo physical parameters are taken as M=1, Du=0.3, Pr=0.71, R=1, Kc=0, Q=0.5, Sc=0.22, λ_1= λ_2=0.5.

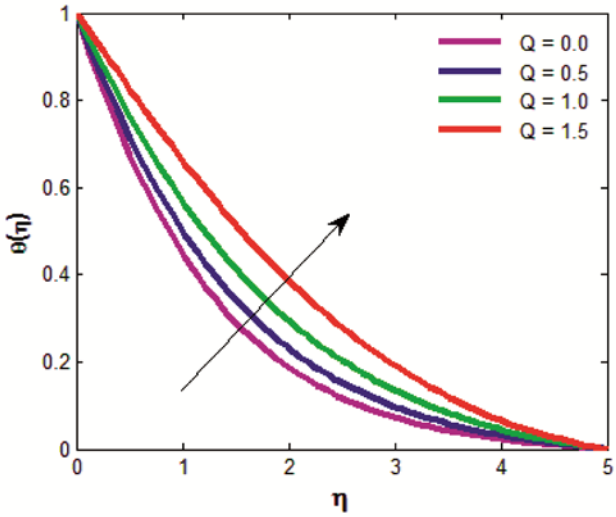

Fig. 12 — For distinct values of Q the temperature distributionin which the values of thermo physical parameters are taken as M=1, Du=0.3, Sr=0.5, Pr=0.71, R=1, Kc=0, Sc=0.22, λ_1= λ_2=0.5.

heat enhances. Figure 12 illustrates the temperature profile of the distinct values of the Q, which indicates that when Q enhances, temperature increases significantly.

The results on heat and mass phenomena for distinct values of magnetic parameter M are determined and graphically displayed in Figs 13 and 14, in the presence of additional parameters used in the analysis. It can be seen that as the value of M raise, the heat as well as mass raises. The motive after it is the force resisting the fluid velocity due to this some amount of energy reserved which favors enhancing the temperature of fluid and mass throughout the thermal boundary layer. For distinct values of λ_1, concentration distribution is presented in Fig. 15, which shows as $\lambda_1$rises, the fluid concentration decreases. For distinct values of λ_2, concentration distribution is presented in Fig. 16. It shows as λ_2 rises, the fluid concentration decays. Figure 17 demonstrates the mass behavior for distinct values of parameter Kc .We notice that a raise in Kc results in a significant decay in concentration. The velocity significantly increases near the wall, after which the contour is uniformly attenuated to a static value in the free flow. Therefore, the chemical

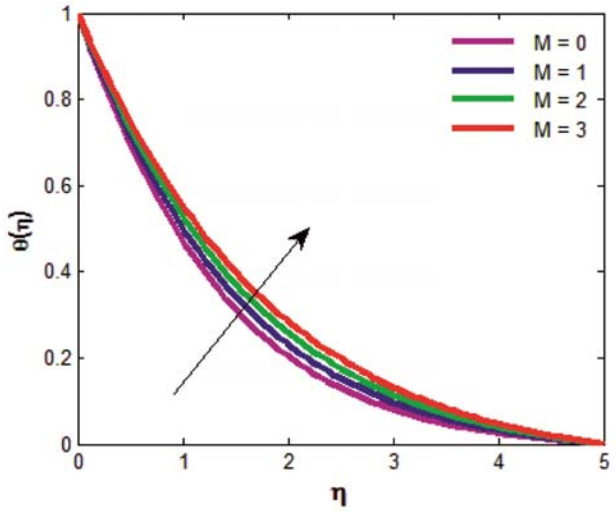

Fig. 13 — For distinct values of M the temperature distribution in which the values of thermo physical parameters are taken as Du=0.3, Sr=0.5, Pr=0.71, R=1, Kc=0, Q=0.5, Sc=0.22, λ_1= λ_2=0.5.

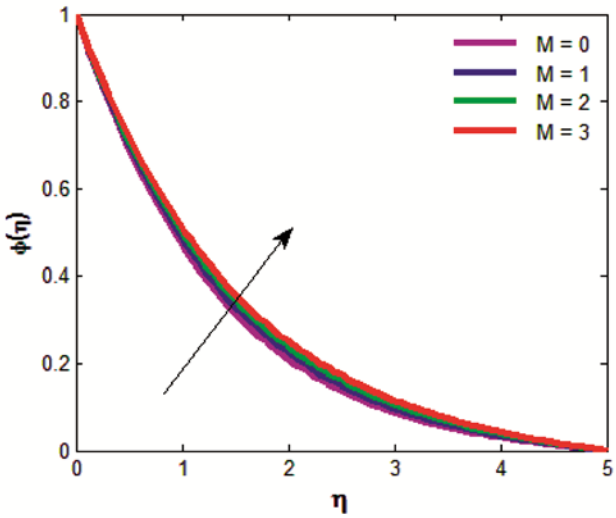

Fig. 14 — For distinct values of M the mass profilein which the values of thermo physical parameters are taken asDu=0.3, Sr=0.5, Pr=0.71, R=1, Kc=0, Q=0.5, Sc=0.22, λ_1= λ_2=0.5.

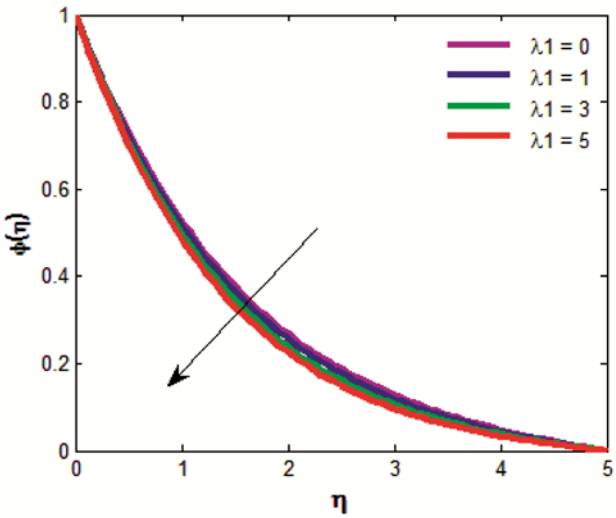

Fig. 15 — For distinct values of λ_1 the mass profilein which the values of thermo physical parameters are taken asM=1, Du=0.3, Sr=0.5, Pr=0.71, R=1, Kc=0, Q=0.5, Sc=0.22, λ_2=0.5.

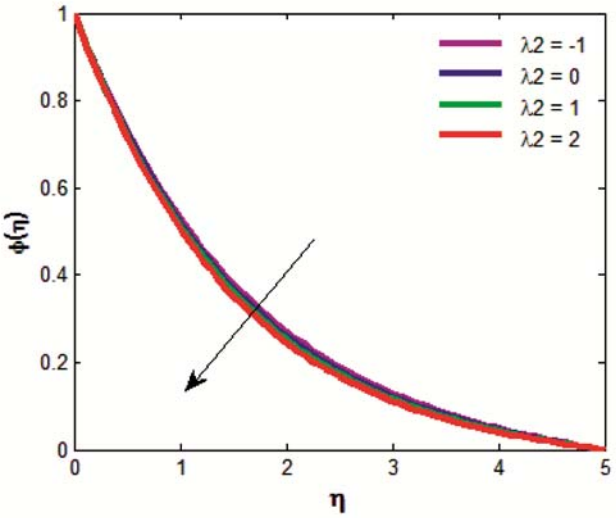

Fig. 16 — For dissimilar values of λ_2 the mass profilein which the values of thermo physical parameters are taken asM=1, Du=0.3, Sr=0.5, Pr=0.71, R=1, Kc=0, Q=0.5, Sc=0.22, λ_1= 0.5.

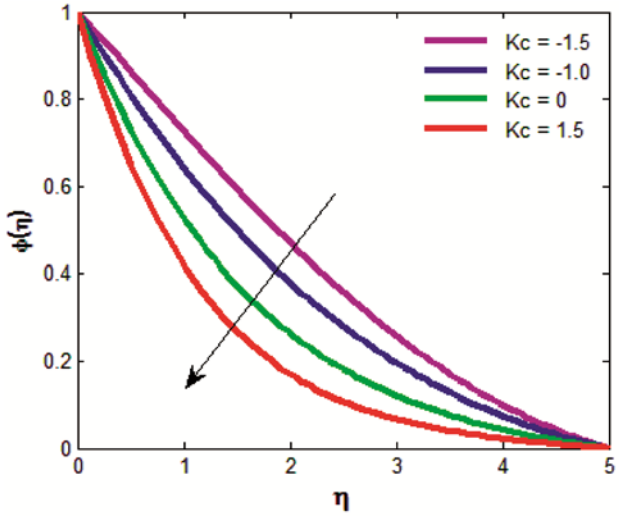

Fig. 17 — For distinct values of λ_2 the mass profilein which the values of thermo physical parameters are taken asM=1, Du=0.3, Sr=0.5, Pr=0.71, R=1, Q=0.5, Sc=0.22, λ_1= λ_2=0.5.

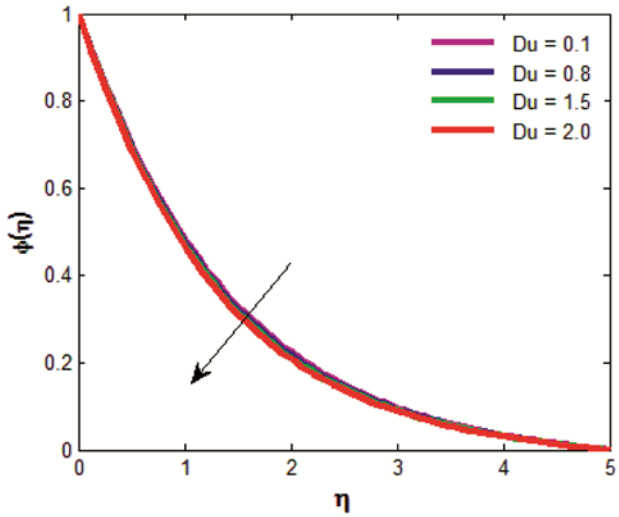

Fig. 18 — For distinct values of Du the concentration distributionin which the values of thermo physical parameters are taken asM=1, Sr=0.5, Pr=0.71, R=1, Kc=0, Q=0.5, Sc=0.22, λ_1= λ_2=0.5.

reaction increases the instantaneous transfer or accelerates the flow. Figure 18 shows the concentration distribution for Dufour parameter and shows that as Du increases, concentration decreases gradually near the vertical heating plate. Figure 19 depicts the massprofile of distinct values of Soret number Sr . We can see a raise in Sr shows, a raise in concentration inside the boundary layer.

7 Conclusions

Free convective flow has been studied in the existence of buoyant force for an electrically

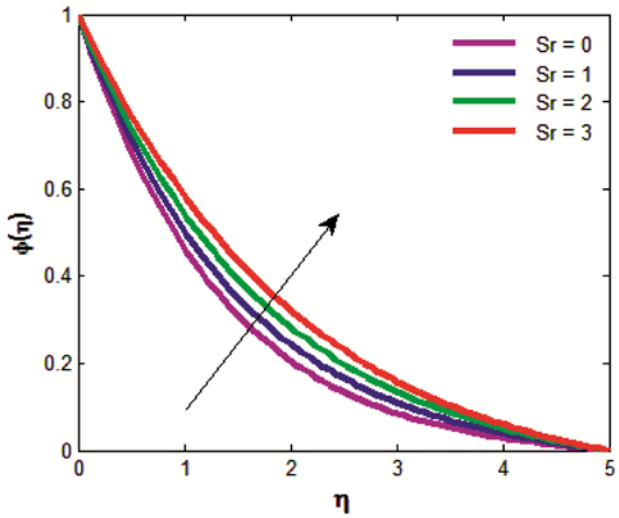

Fig. 19 — For distinct values of Sr the concentration distributionin which the values of thermophysical parameters are taken asM=1, Du=0.3, Pr=0.71, R=1, Kc=0,Q=0.5, Sc=0.22, λ_1= λ_2=0.5.

performing fluid above an extending surface. Space/temperature reliant energy source/sink is considered. To enhance the discussion concentration transfer effect is also taken care of. The numerical solutions of transformed nonlinear coupled ODEs are attained using the Runge-Kutta 4th order method using the shooting method. The following conclusions are noticed from the aforesaid discussion laid down here.

(i) The velocity, temperature function increase, while concentration reduces with the raise in Du.
(ii) The concentration rises, while temperature function reduces with a raise in the Sr.
(iii) The velocity enhances, while concentration reduces with a raise in the λ_1, λ_2
(iv) The velocity and temperature function enhance with the raise in Q.
(v) The velocity reduces with a raise in Pr.
(vi) The velocity reduces while the temperature function increases with the rise in Sc
(vii) The velocity reduces while the temperature and concentration functions increase with the rise in M.
(viii) The concentration reduces with a raise in Kc.

The solution obtained by the present work validates with the previous result obtained by Shivaiah *et al.*[24], Hayat *et al.*[25], Ullah *et al.*[26] in particular cases that deserves the existence of the current work. However, as a concluding remark, the major outcomes of the

present investigation are described as: the buoyant forces overshoot the velocity profile significantly whereas the fluid temperature retards with an increasing Soret number. Finally, the chemical reaction parameter favors retard the concentration profiles resulted in reducing the thickness of the solutal boundary layer.

Nomenclature:

List of Symbols:

υ kinematic viscosity
B_0 strength magnetic field
g acceleration due to gravity
T fluid temperature
T_∞ free stream temperature
T_w wall temperature
T_0 mean temperature
C_0 mean concentration
C solutal concentration
C_∞ free stream concentration
C_w species concentration at the wall
α thermal diffusivity
ρ fluid density
q_r radiative heat flux
σ Stephan-Boltzmann constant,
k^* mean absorption coefficient
Q heat source/sink
k thermal conductivity
D coefficient of mass diffusivity
k_c^* dimensional chemical reaction
$B(x)$ variable magnetic field
Cp specific heat at constant Pressure
U_w stretching velocity
U_0 reference velocity,
L characteristic length,
f non-dimensional stream function
θ non-dimensional temperature
ϕ non-dimensional concentration
M magnetic field parameter
Pr Prandtl number
R thermal radiation
Sc Schmidt number
λ_1 local Thermal Grashof number
λ_2 local Solutal Grashof number
Kc non-dimensional chemical reaction parameter
β_T coefficient of volumetric thermal expansion
β_C coefficient of volumetric solutal expansion
u, v velocity components along x and y directions

References

1 Cortell R, *Phys Lett A*, 372 (5) (2008) 631.
2 Cortell R, *Chem Eng Res Des*, 89 (2011) 85.
3 Ibrahim F S, Elaiw A M & Bakar A A, *Commun Nonlinear Sci Numer Simul*, 13 (2008) 1056.
4 Shateyi S, *J Appl Math*, 2008 (2008) 12.
5 Shateyi S, Motsa S S, *Math Probl Eng*, 2009 (2009) 13.
6 Sakiadis B C, *AIChE J*, 5 (1961) 26.
7 Karthikeyan S, Bhuvaneswari M, Sivasankaran S & Rajan S, *J Appl Fluid Mech*, 9 (2016) 1447.
8 Reddy P S & Chamkha A J, *J Appl Fluid Mech*, 9 (2016) 2443.
9 Gbadeyan J A, Oyekunle T L, Fasogbon P F & Abubakar J U, *J Taibah Univ Sci*, 12 (2018) 631.
10 Bhattacharyya K, Layek G C & Seth G S, *Phys Scr*, 89 (2014) 095203.
11 Mishra S R, Baag S & Mohapatra D K, *Eng Sci Technol Int J*, 19 (2016) 1919.
12 Sharma R P & Mishra S R, *Int J Phys Sci*, 20 (2017) 273.
13 Sharma R P, Ibrahim S M, Jain M & Mishra S R, *Indian J Pure Appl Phys*, 56 (2018) 732.
14 Shamshuddin M, Thumma T & Mishra S R, *Defect Diffus Forum* 392 (2019) 42.
15 Chamkha A J, Mallikarjuna B, Vijaya R B & Rao D R V P, *Int J Numer Method H*, 24 (2014) 1405.
16 Zheng L, Jin X, Zhang X & Zhang J, *Acta Mech Sinica*, 29 (2013) 667.
17 Bishwa R S & Aich A, *IOSR JM*, 12 (2016) 53.
18 Uwanta I J & Usman H, *Int Sch Res Not*, 2014 (2014).
19 Eldabe N & Zeid M A, *J Appl Maths*, 2013 (2013).
20 Moorthy M B K & Senthilvadivu K, *J Appl Maths*, 2012 (2012).
21 Vedavathi N, Ramakrishna K & Reddy K J, *Ain Shams Eng J*, 6 (2015) 363.
22 Sharma R P, Jha A K & Gaur P K, *RMS-Lecture Not Ser*, 21 (2015) 147.
23 Partha M K, *Heat Mass Trans*, 44 (2008) 969.
24 Shivaiah S & Rao J A, *J Naval Arch Marine Eng*, 8 (2011) 37.
25 Hayat T, Nasir T, Khan M I & Alsaedi A, *Res Phys*, 8 (2018) 1017.
26 Ullah I, Khan I & Shafie S, *Sci Rep*, 7 (2017) 1113.

27 Gorla R S R, Encyclopedia fluid mechanics, Advances in flows dynamics,Texas (USA), Gulf Publishing, 1993.
28 Gaffar S A, Prasad V R, Reddy E K & Be´g O A, *Ain Shams Eng J*, 6 (2015) 1009.
29 Hsiao C, Chang W, Char M & Tai B, *Appl Math Comput*, 244 (2014) 390.
30 Chapman S & Cowling T G, The Mathematical Theory of Non-uniform Gases. (Texas (USA), Cambridge University Press), 2nd Edn, 1952.
31 Bhatti M M, Mishra S R, Abbas T & Rashidi M M, *Neural Comput Appl*, 30 (2018) 1237.